Bachelor's Thesis

The influence of excited atomic states in multiphoton ionization

Johannes Porsch

Supervised by:
apl. Prof. Vladislav Yakovlev
Prof. Ulrich Schollwöck

July 12, 2025

Bachelorarbeit

Der Einfluss angeregter atomarer Zustände auf die Mehrphotonenionisation

Johannes Porsch

FAKULTÄT FÜR PHYSIK

July 12, 2025

Supervisor:
apl. Prof. Vladislav Yakovlev
Prof. Ulrich Schollwöck

Abstract

Multiphoton ionization of atoms in strong laser fields is a fundamental process in attosecond physics. In this work, we extend the strong-field approximation (SFA) by incorporating the influence of excited atomic states on ionization rates. Standard SFA formulations neglect these excited states, assuming that the laser field has no effect on the atom before ionization. However, in intense few-cycle laser pulses, the Stark shift and transient population of excited states can significantly modify ionization dynamics. We numerically solve the time-dependent Schrödinger equation (TDSE) using the tRecX code to extract time-dependent probability amplitudes for hydrogen's ground and excited states. These amplitudes are then integrated into the SFA formalism to evaluate their impact on ionization rates.

Contents

List of Figures

1. Introduction

Ionization with an intense laser is one of the most fundamental processes in attosecond physics and quantum mechanics in general and has a broad range of applications such as medical physics or . Weither you want your system to ionize or not, it may be important to understand, how ionization works. However since it is a quantum mechanical process, one has to first ask what information are even experimentally acessible. Quantum mechanics at its very fundamental level tells us one can only measure probabilities and how likely the electron get ionized. Unfortunately, in an actual experiment thats the only option you got. Further one likes to know more about the "path" the electron takes after it gets struck by the laser pulse i.e the response of the electron to the laser pulse. Everytime you hear "path" in quantum mechanics, the first name to think of is Heisenberg. His uncertainty principle sets the boundaries for these type of questions and does not let measure all the information you wish to had. Further to see the electrons path, one has to probe the system just as lightwaves probe the matter around you letting you see. However probing a quantum mechanical system effectively changes the quantum mechanical state of the electron so eventually one has to restrict oneself to something different.

The challenge of a theoretical model is now to predict ionization propabilities and further explain the underlying mechanisms and in the best case allowing some insights what happens between initial state of the atom and measured electron. A clever way to do this is by establishing the concept of an instantanious ionization rate (IIR) via the propertry $P_{\text{ion}} = \int_{\mathbb{R}} \Gamma(t) \mathrm{d}t$. At first sight, "instantanious" seems to conflict with the energy time uncertainty relation $\Delta E \Delta t \geq \hbar/2$. However, instantanious refers to the response of the electron to the laser field, not the and does not contain eny infromation on when exactly does the electron get ionized.

Lets make an example to show how an IIR can be beneficial. Suppose a measurement is made, a laser pulse hits an atom and the outcome is measured, so if the electron is ionized or not. Suppose the measurement is repeated sufficiently many times, one can define a ionization propability for instance 1%. An IIR now allows to investigate which parts of the laser pulse causes what effects in the total ionization propability. One could say, an IIR tells us how likely the electron gets ionized within a certain time interval but of course

averaged over all the measurements made. Note that the IIR does not tell us the electron will get ionized at a certain time because this would violate the energy time uncertainty relation, the value of Γ at a certain time does not have any physical interpretation.

This concept allows us to investigate the ionization process better and understand more about the underlying mechanisms such as defining different limits and regimes (2.4) or make use of the IIR by sampling a light pulse [11]. Due to the challange that the IIR is not really an quantum mechanical observable, it is difficult to have a working notion of it that works for different systems and laser pulses. Eventually one has to start from scratch and derive the IIR from the time dependent schroedinger equation (TDSE) and varios approximations. One approximation most used in this context is called Strong field aproximation (SFA) mostly for its simplicity and the capability to derive ionization rates [2]. However, SFA has its limitations, especially when it comes to comparing ab initio ionization propabilities, i.e. to numerical solutions of the TDSE using dedicated numerical solver. An implicit assumption often made while using SFA is that the laser field has no effect on the atom until the moment of ionization, effectively neglecting excited atomic states. In principle this does not have anything to do with the SFA itself, making it a possible solution to the differences between SFA and ab initio ionization propabilities. This is one of the main goal of this thesis, investigate if the differences from SFA and ab initio ionization propabilities can be explained by the neglect of excited states. Further one would like to investigate the dynamics and effects of the electron before it gets ionized and how they contribute to the ionization dynamics. Particulary important would be to know what matters more, the stark shift or the distortion of the ground state wavefunction. That could lead to an improvement to existing rates, making them besser applicable in the cases mentioned before.

To achieve this, one has to review how the SFA was made previously and how it can be improved (Chapter 2). Later I will implement the extended SFA rate (Chapter 4) and compare the results with existing SFA rates and ab initio ionization propabilities (Chapter 5).

2. Theory

The structure of this chapter largely follows [6], with several modifications and adaptations to the context of this thesis.

The aim of this chapter is to derive an expression for the instantaneous ionization rate (IIR) by solving the time-dependent Schrödinger equation (TDSE) within the framework of the strong-field approximation (SFA).

2.1 Basic Formalism

The goal is to describe the time evolution of a quantum system under an external, time-dependent electromagnetic field in a form suitable for the strong-field approximation. To achieve this, a working formalism must be developed. The starting point is the time-dependent Schrödinger equation for a given Hamiltonian and the Maxwell equations, from which the light-matter interaction can be derived.

2.1.1 Schrödinger Equation

The time evolution of a quantum system $|\Psi(t)\rangle$ is determined by the time-dependent Schrödinger equation, a partial differential equation that describes the relationship between the change in time of $|\Psi(t)\rangle$ with a general Hamiltonian $\mathcal{H}(t)$:

$$i\hbar\frac{\partial}{\partial t}|\Psi(t)\rangle \stackrel{\text{a.u.}}{=} i\frac{\partial}{\partial t}|\Psi(t)\rangle = \hat{\mathcal{H}}(t)|\Psi(t)\rangle. \tag{2.1}$$

$\hat{\mathcal{H}}$ contains all relevant information for the time evolution, meaning it can be understood as being generated by the Hamiltonian. The formal solution of (2.1) depends on the time dependence of the Hamiltonian and the physical system under consideration. In the general case where the Hamiltonian does not commute with itself at different times, the solution

to (2.1) can be written as a Dyson series:

$$|\Psi(t)\rangle = \hat{\mathcal{U}}(t, t_0) |\Psi(t_0)\rangle = \hat{1} + \sum_{n=1}^{\infty} (-i)^n \int_{t_0}^{t} \mathrm{d}t_1 \int_{t_0}^{t_1} \mathrm{d}t_2 \cdots \int_{t_0}^{t_{n-1}} \mathrm{d}t_n \hat{\mathcal{H}}(t_n)\hat{\mathcal{H}}(t_{n-1}) \cdots \hat{\mathcal{H}}(t_1) |\Psi(t_0)\rangle .$$

$$(2.2)$$

Physical setting   The physical setting is a Hydrogen atom in the ground state that is impinged with a high energetic femtosecond laser pulse. The coulomn potential is gi en by

$$\hat{\mathcal{H}}_{\mathrm{C}} = \frac{1}{|x - x_0|}.$$

Further the hamiltonian can be partitioned into seperate parts since the TDSE is linear. For instance in the the ground state part and the interaction part:

$$\hat{\mathcal{H}}(t) = \frac{\hat{\mathbf{P}}^2}{2m} + \hat{\mathcal{H}}_{\mathrm{C}} + \hat{\mathcal{H}}_{\mathrm{I}}(t).$$

2.1.2   Light-Matter Interaction

A light wave consists of an electric field $\mathbf{E}(\underline{x}, t)$ and a magnetic field $\mathbf{B}(\underline{x}, t)$, which propagate through vacuum at the speed of light. These fields are defined by Maxwell's equations in empty space:

$$\nabla \cdot \mathbf{E} = 0 \qquad \nabla \times \mathbf{E} = -\frac{\partial \mathbf{B}}{\partial t}$$
$$\nabla \cdot \mathbf{B} = 0 \qquad \nabla \times \mathbf{B} = \mu_0 \epsilon_0 \frac{\partial \mathbf{E}}{\partial t}$$

These equations can be solved using the potentials

$$\mathbf{E} = -\nabla\varphi - \frac{\partial \mathbf{A}}{\partial t},$$
$$\mathbf{B} = \nabla \times \mathbf{A},$$

$$(2.3)$$

where $\mathbf{A}(\underline{x}, t)$ is the vector potential and $\varphi(\underline{x}, t)$ is the scalar potential. These potentials are not uniquely determined, as different choices can lead to the same physical fields. Specifically, the transformations

$$\mathbf{A} \to \mathbf{A} + \nabla\chi, \; \varphi \; \to \varphi - \frac{\partial \chi}{\partial t},$$

$$(2.4)$$

with $\chi(t)$ being an arbitrary smooth scalar function, also satisfy Maxwell's equations. This non-uniqueness is referred to as gauge freedom and arises directly from the structure of the equations. Selecting a particular gauge (i.e., fixing a certain χ) can be just a matter of convenience and simplify calculations, as demonstrated below.

2.1.3 Dipole Approximation

The dipole approximation is a widely used simplification in light-matter interaction. It applies when the wavelength of the optical field is significantly larger than both the size of the relevant bound electron states and the maximum displacement of a free electron. Additionally, it assumes that the magnetic field of the light has a negligible effect on the electron dynamics, requiring nonrelativistic particle velocities.

To derive this approximation, we first express Maxwell's equations in terms of the vector and scalar potentials, as defined in (2.3). This results in two coupled differential equations, which complicates the analysis. However, a simpler expression for the vector potential $\mathbf{A}$ can be obtained by selecting a specific gauge—the Lorentz gauge:

$$\partial_\mu \mathbf{A}^\mu = 0 \quad \text{or} \quad \nabla \cdot \mathbf{A} + \frac{\partial \varphi}{\partial t} = 0.$$

This gauge choice is achieved by solving the inhomogeneous wave equation for χ, which arises in the explicit calculation and is feasible when $\mathbf{A}$ and φ are known. With this gauge, Maxwell's equations decouple into:

$$\nabla^2 \varphi - \frac{\partial^2 \varphi}{\partial t^2} = 0,$$

$$\nabla^2 \mathbf{A} - \frac{\partial^2 \mathbf{A}}{\partial t^2} = 0.$$

The second equation is of particular interest, as it is a wave equation describing plane-wave solutions for $\mathbf{A}$:

$$\mathbf{A}(\underline{x}, t) = \mathbf{A}_0 \mathrm{e}^{\pm i(\underline{k} \cdot \underline{x} - \omega t)}.$$

Mathematically, the dipole approximation corresponds to the leading-order term in the Taylor expansion of $\mathrm{e}^{i\underline{k} \cdot \underline{x}}$. Consequently, the vector potential becomes spatially independent and can be approximated as [5]:

$$\mathbf{A}(\underline{x}, t) = \mathbf{A}_0 \mathrm{e}^{\mp i\omega t} \exp\left\{ \pm 2\pi i \frac{|\underline{x}|}{\lambda} \underline{e}_k \cdot \underline{e}_x \right\} \approx \mathbf{A}_0 \mathrm{e}^{\mp i\omega t} \left(1 + \mathcal{O}\left(\frac{|\underline{x}|}{\lambda} \right) \right) = \mathbf{A}(t)$$

This approximation holds as long as the wavelength is sufficiently large. Under these conditions, the magnetic field simplifies to:

$$\mathbf{B} = \nabla \times \mathbf{A} \approx 0.$$

Although a different gauge may be chosen later, the physical description of the system remains unchanged. The dipole approximation itself is gauge-independent, ensuring that $\mathbf{B}$

remains approximately zero in any gauge. The Lorentz gauge is used here for convenience, as it provides an intuitive framework for the vector potential expansion.

The dipole approximation is valid for most experimental configurations, including the calculations in this work. However, it has limitations—for example, it breaks down in cases where strong-field ionization generates very fast electrons ([5], [10]).

This was the essence of the dipole approximation. To further simplify the description of the laser field in the Hamiltonian, the choice of gauge must be considered more carefully.

2.1.4   Gauges

Calculating ionization rates in strong-field physics presents challenges due to the choice of gauge. While gauge transformations do not alter physical reality in classical electrodynamics, they can affect the practical computation of formulas derived in this chapter, requiring careful consideration.

First, we derive two basic expressions for the Hamiltonian in the velocity gauge and length gauge using the dipole approximation. The semiclassical Hamilton function for a free electron in an electric field[1] is:

$$\hat{\mathcal{H}}(\underline{x}, t) = \frac{1}{2m}(\hat{\mathbf{P}} - e\mathbf{A}(\underline{x}, t))^2 - e\varphi(\underline{x}, t) \tag{2.5}$$

Under the dipole approximation, this simplifies to:

$$\hat{\mathcal{H}}(\underline{x}, t) = \frac{\hat{\mathbf{P}}^2}{2m} - \frac{e}{m}\hat{\mathbf{P}} \cdot \mathbf{A}(t) + \frac{e^2}{2m}\mathbf{A}^2(t) - e\varphi(\underline{x}, t)$$

In most literature, φ is set to zero at this stage of the derivation because the sources of the electromagnetic wave lie outside the region of interest. While the dipole approximation does not strictly necessitate this assumption, φ will be left as is.

A common assumption in semiclassical Hamiltonians is that the vector potential alone drives electron state transitions, with no back-reaction from the electron [5]. This approximation holds for sufficiently high laser intensities, though its validity may depend on specific conditions.

Next, we perform a gauge transformation called length gauge via:

$$\chi = -\mathbf{A}(t) \cdot \underline{x} \tag{2.6}$$

---

[1]Derivation can be found in [9]

This transformation sets $\mathbf{A}$ to zero, modifying φ as follows:

$$\nabla \varphi \to \nabla \cdot (\varphi + \mathbf{x} \cdot \frac{\partial \mathbf{A}}{\partial t}) = \nabla \varphi + \frac{\partial \mathbf{A}}{\partial t} = -\mathbf{E} \tag{2.7}$$

Integrating this equation from the origin to $\mathbf{x}$ yields the electric potential in the length gauge. With $\mathbf{r}$ now quantized, the Hamiltonian becomes:

$$\hat{\mathcal{H}}(\underline{x}, t) = \frac{\hat{\mathbf{P}}^2}{2m} - e\hat{\mathbf{x}} \cdot \mathbf{E}$$

The time-dependent part $\hat{\mathcal{H}}(t)$ of the Hamiltonian can be expressed as:

$$\hat{\mathcal{H}}_{\mathrm{L}}(t) = -\hat{\mathbf{d}} \cdot \mathbf{E}(t) \tag{2.8}$$

where $\hat{\mathbf{d}} = e\hat{\mathbf{x}}$ is the dipole operator and $\mathbf{E}(t)$ is the electric field.

An alternative gauge transformation, the velocity gauge, is also relevant. Using:

$$\chi = -\frac{e^2}{2m} \int_{-\infty}^{t} \mathbf{A}^2(t')\mathrm{d}t'$$

the dipole approximation leaves $\mathbf{A}$ unchanged but modifies φ as:

$$\varphi \to \varphi - \frac{e^2}{2m}\mathbf{A}^2(t)$$

resulting in the Hamiltonian:

$$\hat{\mathcal{H}}(\underline{x}, t) = \frac{\hat{\mathbf{P}}^2}{2m} - \frac{e}{m}\hat{\mathbf{P}} \cdot \mathbf{A}(t)$$

and

$$\hat{\mathcal{H}}_{\mathrm{V}}(t) = -\frac{e}{m}\hat{\mathbf{P}} \cdot \mathbf{A}(t) \tag{2.9}$$

where φ is set to zero.

These are standard formulations of the interaction Hamiltonian for light-matter interactions. As with any gauge transformation, certain scenarios favor one gauge over another (see Chapter 4).

2.2 Strong Field Approximation

The difficulty with ionization arises from the existence of in some sense two Hilbert spaces: one for the bound states in the Hydrogen atom that accounts for distortion of the wavefunction due to the laser field, and another for the continuum states that are primarily

affected by the laser field but also influenced by the binding potential.

It will be shown that SFA provides a treatment for the second Hilbert space, simplifying its description. However, previous SFA formulations oversimplify the first Hilbert subspace to such an extent that there remains one Hilbert space for eigenstates unaffected by the laser field and another for continuum states unaffected by the binding potential.

SFA, in principle, concerns only the second part; neglecting the dynamics before ionization is not truly part of it. This section derives an expression that avoids excessive simplification of the first Hilbert space. Additionally, it will be demonstrated that there are two equivalent ways of solving the TDSE, which later diverge when approximations are introduced. Nevertheless, it becomes evident that these approaches nevertheless yield the same analytical result.

2.2.1   Subspaces

The full time-dependent Hamiltonian $\hat{\mathcal{H}}(t)$ is projected onto subspaces using projection operators defined by:

$$\hat{X} = \sum_n |\Psi_n\rangle\langle\Psi_n| \quad \text{and} \quad \hat{Y} = \hat{1} - \hat{X}$$

The use of projection operators for this type of problem is inspired by [12]. Projection operators are idempotent, i.e. $\hat{X}^2 = \hat{X}$. This property can be considered as the defining characteristic of projection operators, so applying them twice produces nothing new.

Here, $|\Psi_n\rangle$ represents the bound states of the atom. Using $\hat{X} + \hat{Y} = \hat{1}$, any partition of the Hamiltonian can be chosen. The most natural partitioning is first written as:

$$\hat{\mathcal{H}}(t) = \underbrace{\hat{X}\hat{\mathcal{H}}(t)\hat{X}}_{\hat{\mathcal{H}}^{\mathrm{XX}}(t)=\hat{\mathcal{H}}_0^{\mathrm{ODE}}(t)} + \underbrace{\hat{Y}\hat{\mathcal{H}}(t)\hat{Y} + \hat{X}\hat{\mathcal{H}}(t)\hat{Y} + \hat{Y}\hat{\mathcal{H}}(t)\hat{X}}_{\hat{\mathcal{H}}^{\mathrm{YY}}(t)+\hat{\mathcal{H}}^{\mathrm{XY}}(t)+\hat{\mathcal{H}}^{\mathrm{YX}}(t)=\hat{\mathcal{H}}_{\mathrm{I}}^{\mathrm{ODE}}(t)} = \hat{\mathcal{H}}_0^{\mathrm{ODE}}(t) + \hat{\mathcal{H}}_{\mathrm{I}}^{\mathrm{ODE}}(t)$$

Similar to $\hat{\mathcal{H}}(t) = \hat{\mathcal{H}}_0(t) + \hat{\mathcal{H}}_{\mathrm{I}}(t)$, where $\hat{\mathcal{H}}_{\mathrm{I}}(t)$ represents the interacting perturbation (for instance, in the length gauge (2.8)), but now applied to the full Hamiltonian projected onto subspaces. For reasons that will be explained later, this is referred to as the ODE partition. The acronym ODE (Ordinary Differential Equation) reflects its later use in solving for the coefficients that weight the wavefunction. While the notation may appear arbitrary now, its significance will become clear later.

The Hamiltonian can alternatively be partitioned into a different form:

$$\hat{\mathcal{H}}(t) = \underbrace{\hat{X}\hat{\mathcal{H}}(t)\hat{X} + \hat{Y}\hat{\mathcal{H}}(t)\hat{Y} + \hat{X}\hat{\mathcal{H}}(t)\hat{Y}}_{\hat{\mathcal{H}}^{\mathrm{XX}}(t)+\hat{\mathcal{H}}^{\mathrm{YY}}(t)+\hat{\mathcal{H}}^{\mathrm{XY}}(t)=\hat{\mathcal{H}}_0^{\mathrm{tRecX}}(t)} + \underbrace{\hat{Y}\hat{\mathcal{H}}(t)\hat{X}}_{\hat{\mathcal{H}}^{\mathrm{YX}}(t)=\hat{\mathcal{H}}_{\mathrm{I}}^{\mathrm{tRecX}}(t)} = \hat{\mathcal{H}}_0^{\mathrm{tRecX}}(t) + \hat{\mathcal{H}}_{\mathrm{I}}^{\mathrm{tRecX}}(t)$$

The physical meaning of these terms can be interpreted as follows: In $\hat{\mathcal{H}}^{\mathrm{XX}}(t)$, the

electron remains within the subspace and can always be described by a superposition of bound states. Without ionization, this would be the only term governing the time evolution. In previous work, this part of the Hamiltonian was often simplified to the extent that effects like Stark shift or coupling to excited states were neglected.

$\hat{\mathcal{H}}^{\mathrm{YY}}(t)$ describes similar dynamics, but in the subspace of continuum states rather than bound states. While in reality these two spaces cannot be completely separated, this distinction provides conceptual clarity. This is the part where the SFA will later be applied.

The remaining terms describe different physical processes. Two processes can occur: ionization of the electron or recombination with the atom. These processes are governed by the terms $\hat{\mathcal{H}}^{\mathrm{XY}}(t)$ and $\hat{\mathcal{H}}^{\mathrm{YX}}(t)$. In the present case, only one of these terms is relevant, and it will be shown later that $\hat{\mathcal{H}}^{\mathrm{YX}}(t)$ is responsible for ionization, effectively "kicking" the electron out of the atom [6].

While this approach may initially appear unnecessary, it establishes boundaries for the electron's behavior and provides useful intuition.

2.2.2   Dyson equation

For determining the time evolution, care must be taken since the full Hamiltonian does not commute with itself at different times, requiring an exact treatment. As the full Dyson series (2.2) can be cumbersome to deal with, an alternative approach is used. This approach is enabled by the fact that the Hamiltonian can be split into two parts by projecting it into subspaces. The ansatz chosen here is with the Dyson equation. It relies on the time evolution operator and is completely equivalent to the TDSE and therefore to the Dyson series (2.2). It can be written in two forms that are equivalent in their raw formulation but may yield different results when approximations such as SFA are introduced.

The more intuitive form of the Dyson equation for this physical setting is given by:

$$\hat{\mathcal{U}}(t, t_0) = \hat{\mathcal{U}}_0^{\mathrm{ODE}}(t, t_0) - i \int_{t_0}^{t} \hat{\mathcal{U}}(t, t') \hat{\mathcal{H}}_{\mathrm{I}}^{\mathrm{ODE}}(t') \hat{\mathcal{U}}_0^{\mathrm{ODE}}(t', t_0) \mathrm{d}t' \tag{2.10}$$

Note that the ODE propagators are not identical to the tRecX propagators (2.11), but within the Dyson ansatz, the full propagator $\hat{\mathcal{U}}$ remains unchanged. This will change later when SFA is introduced. Most formulas in this thesis can be best read from right to left, such as this one. The time evolution starts with the Hamiltonian projected onto the bound states. The interaction Hamiltonian then effectively ionizes the electron, inducing a transition to a virtual state, followed by propagation with the full time evolution. For more insights, refer to [6].

The Dyson equation can also be expressed in a slightly different form:

$$\hat{\mathcal{U}}(t,t_0) = \hat{\mathcal{U}}_0^{\text{tRecX}}(t,t_0) - i \int_{t_0}^t \hat{\mathcal{U}}_0^{\text{tRecX}}(t,t')\hat{\mathcal{H}}_I^{\text{tRecX}}(t')\hat{\mathcal{U}}(t',t_0)\mathrm{d}t' \tag{2.11}$$

It can be verified that both equations satisfy the TDSE by direct substitution of $\hat{\mathcal{U}}(t,t_0)$. The main difference between the tRecX and ODE formulations is that the "initial" propagator on the right side is now the full time propagator instead of a reduced one.

To simplify the analysis, the physical setting is further specified. Starting from the ground state of the atom, the time evolution is given by $\hat{\mathcal{U}}(t,t_0)|\Psi_0(t_0)\rangle$. For additional simplification, a projection onto a continuum state $|\Pi(t_c)\rangle$ at time t_c is considered. $|\Pi(t_c)\rangle$ does not represent a plane wave but rather an abstract state characterized by its momentum. Naturally, there is no overlap between $|\Pi(t_c)\rangle$ and $\hat{\mathcal{U}}_0^{\text{ODE}}(t,t_0)|\Psi_0(t_0)\rangle$ or with $\hat{\mathcal{U}}_0^{\text{tRecX}}(t,t_0)|\Psi_0(t_0)\rangle$, as the electron has not yet been ionized and no initial population in the continuum is assumed [6]. Furthermore, when $\hat{\mathcal{H}}_I^{\text{ODE}}(t')$ and $\hat{\mathcal{H}}_I^{\text{tRecX}}(t')$ are expanded, and the orthogonality of bound states and continuum states is taken into account, most terms of $\hat{\mathcal{H}}_I(t')$ vanish. The remaining expressions are:

$$\langle\Pi(t_c)|\hat{\mathcal{U}}_0^{\text{ODE}}(t,t_0)|\Psi_0(t_0)\rangle\rangle = -i\int_{t_0}^t \langle\Pi(t_c)|\hat{\mathcal{U}}(t,t')\hat{Y}\hat{\mathcal{H}}(t')\hat{X}\hat{\mathcal{U}}_0^{\text{ODE}}(t',t_0)|\Psi_0(t_0)\rangle\,\mathrm{d}t' \tag{2.12}$$

and

$$\langle\Pi(t_c)|\hat{\mathcal{U}}_0^{\text{tRecX}}(t,t_0)|\Psi_0(t_0)\rangle\rangle = -i\int_{t_0}^t \langle\Pi(t_c)|\hat{\mathcal{U}}_0^{\text{tRecX}}(t,t')\hat{Y}\hat{\mathcal{H}}(t')\hat{X}\hat{\mathcal{U}}(t',t_0)|\Psi_0(t_0)\rangle\,\mathrm{d}t' \tag{2.13}$$

Note: No approximations have been made; (2.12) and (2.13) are exact.

2.2.3 Strong Field Approximation

In principle, the strong field approximation (SFA) involves neglecting the binding potential after ionization. This approximation is intuitively reasonable because the laser field becomes the dominant force acting on the electron, exerting significantly greater influence on the ionization dynamics than the Coulomb potential. It should be noted that SFA is not restricted to high-intensity laser pulses; even for small ionization probabilities (e.g., <0.01), SFA implies that once ionization occurs, the laser pulse dominates the subsequent dynamics.

First, the ODE partitioning must be addressed. The time evolution operator after ionization can be expressed as:

$$\hat{\mathcal{U}}(t,t') \approx \hat{\mathcal{U}}_{\text{SFA}}(t,t') = e^{-i\int_{t'}^t \hat{\mathcal{H}}_{SFA}(t'')\mathrm{d}t''} \quad \text{and} \quad \mathcal{H}_{\text{SFA}}(t') = \hat{\mathcal{H}}(t) - \hat{\mathcal{H}}_C$$

Similarly, for the tRecX partitioning:

$$\hat{\mathcal{U}}_0^{\text{tRecX}}(t,t') \approx \hat{\mathcal{U}}_{\text{SFA}}(t,t') = e^{-i\int_{t'}^{t}\hat{\mathcal{H}}_{SFA}(t'')dt''} \quad \text{and} \quad \mathcal{H}_{\text{SFA}}(t') = \hat{\mathcal{H}}(t) - \hat{\mathcal{H}}_{\text{C}}$$

An exact expression for the SFA time evolution operator can be written, as it now commutes with itself at different times.

The SFA is particularly useful because the eigenstates of $\hat{H}_{\text{SFA}}$ have an exact analytical solution: the Volkov states. To see this, consider the semiclassical Hamiltonian in (2.5).

Classically, the physics driven by the momentum operator $\hat{\mathbf{P}}$ is known as the canonical momentum, given by:

$$\frac{\partial \mathcal{L}}{\partial \dot{\underline{x}}} = \underline{P} = m\dot{\underline{x}} + \frac{e}{c}\mathbf{A} \overset{\text{a.u.}}{=} \mathbf{p} + \mathbf{A} \tag{2.14}$$

where $\mathcal{L}$ is the Lagrangian of the system.

In this case, the canonical momentum is conserved. To verify this, setting $\varphi = 0$ (justified earlier) gives $\mathbf{E} = -\frac{\partial \mathbf{A}}{\partial t}$. The equation of motion for a charged particle in an electromagnetic field [9] is:

$$\frac{d\mathbf{p}}{dt} = \mathbf{E} + (\dot{\underline{x}} \times \mathbf{B}) \approx -\frac{\partial \mathbf{A}}{\partial t} = -\frac{d\mathbf{A}}{dt}$$

Thus, $\frac{d}{dt}\mathbf{P} = 0$.

And also the energy of the system is clear:

$$E(t) = \dot{\mathbf{x}}\frac{\partial \mathcal{L}}{\partial \dot{\mathbf{x}}} - \mathcal{L} = \frac{\mathbf{p}^2}{2} \tag{2.15}$$

Note that the energy is not conserved, as the previous argument holds only for the canonical momentum, not the kinetic momentum.

The key observation is that $\langle \Pi(t_{\text{c}})|$ (not $\langle \mathbf{p}(t_{\text{c}})|$!) is an eigenstate of $e^{-i\int_{t'}^{t}\hat{H}\text{SFA}(t'')dt''}$. Combining (2.14) and (2.15) yields:

$$\langle \Pi(t_c)|\,e^{-i\int_{t'}^{t}\hat{\mathcal{H}}_{SFA}(t'')dt''} = \langle \Pi(t_c)|\,e^{-i\int_{t'}^{t}(\underline{P}-\mathbf{A}(t''))^2 dt''}$$

Here, $\mathbf{P}$ is time-independent, while $\mathbf{A}$ is not.

Using the conservation of canonical momentum, the momentum at other times can be calculated. Of particular interest is the asymptotic limit when the laser field vanishes:

$$\underline{P} = \mathbf{p}(t'') + \mathbf{A}(t'') = \mathbf{p}(t \to \infty) + \mathbf{A}(t \to \infty) = \mathbf{p}$$

Furthermore (how??),

$$|\Pi\rangle = |\underline{P}\rangle = |\mathbf{p} + \mathbf{A}\rangle$$

Combining these results leads to the following expressions for both tRecX and ODE:

$$\langle \Pi(t_{\mathrm{c}})| \hat{\mathcal{U}}_0^{\mathrm{ODE}}(t,t_0) |\Psi_0(t_0)\rangle\rangle = -i \int_{t_0}^{t} e^{-i \int_{t'}^{t} (\underline{P} - \mathbf{A}(t''))^2 \mathrm{d}t''} \langle \mathbf{p} + \mathbf{A}| \hat{\mathcal{H}}(t') \hat{X} \hat{\mathcal{U}}_0^{\mathrm{ODE}}(t',t_0) |\Psi_0(t_0)\rangle \, \mathrm{d}t'$$
(2.16)

and

$$\langle \Pi(t_{\mathrm{c}})| \hat{\mathcal{U}}_0^{\mathrm{tRecX}}(t,t_0) |\Psi_0(t_0)\rangle\rangle = -i \int_{t_0}^{t} e^{-i \int_{t'}^{t} (\underline{P} - \mathbf{A}(t''))^2 \mathrm{d}t''} \langle \mathbf{p} + \mathbf{A}| \hat{\mathcal{H}}(t') \hat{X} \hat{\mathcal{U}}(t',t_0) |\Psi_0(t_0)\rangle \, \mathrm{d}t'$$
(2.17)

Note that the SFA eliminates the difference in the left part of the integrand between ODE and tRecX, making the two equations distinct. The final step introduces a new approximation for $\hat{U}_0^{\mathrm{ODE}}(t',t_0) |\Psi_0(t_0)\rangle$ and $\hat{U}(t',t_0) |\Psi_0(t_0)\rangle$.

ODE   Regardless of the final form, the expression can be expanded in the bound states $|\Psi_n\rangle$. This is clear by considering the defining equation of the time evolution operator and observing that any overlap of $\hat{\mathcal{U}}_0^{\mathrm{ODE}}(t',t_0) |\Psi_0(t_0)\rangle$ with a state outside the bound-state representation would cancel out due to $\hat{X}$. With this consideration, an ansatz using the interaction picture can be formulated as:

$$\hat{\mathcal{U}}_0^{\mathrm{ODE}}(t',t_0) |\Psi_0(t_0)\rangle = \sum_n c_n(t') e^{-iE_n t'} |\Psi_n\rangle$$

The factors $e^{-iE_n t'}$ are factored out to avoid potential numerical issues arising from their rapid oscillations.

In theory, this ansatz is exact but relies on the implicit assumption that the Hilbert spaces can be easily separated. Additionally, it assumes that the bound states remain unaffected by the laser field, which is not strictly true in reality. However, this approximation can be justified by the low laser intensity and the resulting ionization probability not exceeding 0.01.

tRecX   This case involves a more severe approximation. The primary advantage is that only the time evolution up to the ionization moment t' is required. The same assumptions regarding laser intensity and ionization probability apply here, justifying the approximation of the time evolution as a superposition of bound states:

$$\hat{\mathcal{U}}(t',t_0) |\Psi_0(t_0)\rangle = \sum_n c_n(t') e^{-iE_n t'} |\Psi_n\rangle$$

The key difference between the two ansatzes lies in the coefficients $c_n(t')$. In the ODE case, the coefficients are obtained by solving the TDSE within the subspace spanned by

the bound states. This approach effectively cuts off ionization, forcing the electron to the subspace regardless of laser intensity. Implementing this leads to a system of ordinary differential equations for the coefficients, hence the name. In contrast, the tRecX approach is fundamentally different. Here, the TDSE must be solved in the full Hilbert space, with the coefficients extracted at times t'. In the atto/femtosecond regime, this demands substantial computational resources, as the electron exits the sub-Hilbert space during the process. For these numerical simulations, a solver called tRecX (discussed in Chapter 3) was employed, motivating the name.

Unlike other literature ([2], [6]), this ansatz does not neglect transitions between bound states prior to ionization. For example, the laser pulse may excite the electron without immediately ionizing it. The coefficients are expected to capture all relevant dynamics within the hydrogen atom before ionization, including effects such as AC Stark shifts and ground-state distortion.

The final expression can now be presented. By simplifying the dipole matrix element $\mathbf{d}_n(\mathbf{p} + \mathbf{A}) = \langle \mathbf{p} + \mathbf{A} | \hat{\mathcal{H}}(t') | \Psi_n \rangle$ between the bound state and the continuum state, the dipole approximation (2.8) can be applied, yielding:

$$\langle \Pi(t_\mathrm{c}) | \Psi_n(t) \rangle = -\frac{i}{2} \int_{t_0}^{t} e^{-i \int_{t'}^{t} (\underline{P} - A_z(t''))^2 \mathrm{d}t''} E_z(t') \sum_n c_n(t) e^{-iE_n t'} \langle \mathbf{p} + A_z | \hat{d}_z | \Psi_n \rangle \, \mathrm{d}t'$$

Here, the electric field is polarized along the z-axis. This equation corresponds to the strong-field S-matrix in the length gauge, as found in many papers [2], but with the distinction that excited states are not neglected.

2.3 Ionization rates

What is a ionization rate and why do we want to have it?

A dilemma exists in the current approaches: while numerical simulations provide accurate ionization probabilities, they fail to yield ionization rates. Conversely, analytical calculations produce reliable ionization rates but incorrect probabilities (see GASFIR paper).

No experimental method has been developed to directly measure ionization rates - only ionization probabilities, which represent a quantum mechanical observable, can be measured.

When an electromagnetic field is present, projections onto bound/unbound states lead to non-physical gauge-dependent predictions [14]. The tunneling time is imaginary, source???

2.3.1   Derivation of SFA Rate

The derivation mainly follows [2] with some modifications. First, the ionization probability is expressed as the amplitude of projection of the wavefunction onto the continuum subspace. The total ionization probability is obtained by integrating the ionization rate over the time domain. Therefore, the SFA rate (2.2.3) can be written as:

$$\lim_{t \to \infty} \langle \Psi(t)| \int d^3p\, |p\rangle \langle p|\, \Psi(t)\rangle = \int_{-\infty}^{\infty} \Gamma_{\text{SFA}}(t)dt$$

$$= \int d^3p \int_{-\infty}^{\infty} \int_{-\infty}^{\infty} dt_1 dt_2\, e^{\frac{i}{2}\int_{t_1}^{t_2}(\underline{p}+A_z(t''))^2 dt''} E_z(t_1)E_z(t_2)$$

$$\times \left(\sum_n e^{iE_n t_1} c_n^*(t_1) d_{z,n}^*(\underline{p}+A_z(t_1)) \right) \left(\sum_n e^{-iE_n t_2} c_n(t_2) d_{z,n}(\underline{p}+A_z(t_2)) \right)$$

By changing variables to $t = \frac{t_2+t_1}{2}$ and $T = \frac{t_2-t_1}{2}$ and using the fact that the laser pulse is polarized along the z-axis, the expression becomes:

$$\Gamma_{\text{SFA}}(t) = \int d^3p \int_{-\infty}^{\infty} dT\, e^{\frac{i}{2}\int_{t-T}^{t+T}(\underline{p}+A_z(t''))^2 dt''} E_z(t-T)E_z(t+T)$$

$$\times \left(\sum_n e^{i(t-T)E_n} c_n^*(t-T) d_{z,n}^*(\underline{p}+A_z(t-T)) \right) \left(\sum_n e^{-i(t+T)E_n} c_n(t+T) d_{z,n}(\underline{p}+A_z(t+T)) \right)$$

$$= \sum_{n_1} \sum_{n_2} \int_0^{\infty} dp\, p^2 \int_0^{\pi} d\theta_p\, \sin\theta_p \int_0^{2\pi} d\phi_p \int_{-\infty}^{\infty} dT\, e^{\frac{i}{2}\int_{t-T}^{t+T}(\underline{p}+A_z(t''))^2 dt''} e^{i(t-T)E_{n_1} - i(t+T)E_{n_2}}$$

$$\times E_z(t-T)E_z(t+T)c_{n_1}^*(t-T)c_{n_2}(t+T)d_{z,n_1}^*(\underline{p}+A_z(t-T))d_{z,n_2}(\underline{p}+A_z(t+T))$$

The integration variable is changed from $\mathbf{p}$ to $\mathbf{p} + \mathbf{A}$, and with $\boldsymbol{\Delta}(t') = \mathbf{A}(t+t') - \mathbf{A}(t)$, the expression becomes:

$$\sum_{n_1} \sum_{n_2} \int_0^{\infty} dp\, p^2 \int_0^{\pi} d\theta_p\, \sin\theta_p \int_0^{2\pi} d\phi_p \int_{-\infty}^{\infty} dT\, e^{\frac{i}{2}\int_{-T}^{T}(\underline{p}+\Delta_z(t''))^2 dt''} e^{i(t-T)E_{n_1} - i(t+T)E_{n_2}}$$

$$\times E_z(t-T)E_z(t+T)c_{n_1}^*(t-T)c_{n_2}(t+T)d_{z,n_1}^*(\underline{p}+\Delta_z(-T))d_{z,n_2}(\underline{p}+\Delta_z(T))$$

Also the integrand in the exponential function can be further simplifyed:

$$\frac{i}{2}\int_{-T}^{T}(\mathbf{p}+\Delta_z(t''))^2 dt'' = i\mathbf{p}^2 T + \frac{i}{2}\int_{-T}^{T}\Delta_z(t'')^2 + 2\mathbf{p}\cdot\Delta_z(t'')dt''$$

$$= i\mathbf{p}^2 T + ip\cos\theta_p \int_{-T}^{T}\Delta_z(t'')dt'' + \frac{i}{2}\int_{-T}^{T}\Delta_z(t'')^2 dt''$$

Following the notation used in the code as well as in [2], where

$$\bar{\boldsymbol{\Delta}}^k = \int_{-T}^{T}\boldsymbol{\Delta}^k(t')dt' = \int_{-T}^{T}(\mathbf{A}(t+t') - \mathbf{A}(t))^k dt'$$

the final SFA rate to be implemented is given by:

$$\Gamma_{\mathrm{SFA}}(t) = \sum_{n_1} \sum_{n_2} \int_0^\infty \mathrm{d}p\, p^2 \int_0^\pi \mathrm{d}\theta_p \, \sin\theta_p \int_0^{2\pi} \mathrm{d}\phi_p \int_{-\infty}^\infty \mathrm{d}T$$

$$\times \exp\left(i\mathbf{p}^2 T + ip\cos\theta_p \bar{\Delta}_z^k + \frac{i}{2}\bar{\Delta}_z^2 + i(t-T)E_{n_1} - i(t+T)E_{n_2} \right)$$

$$\times E_z(t-T)E_z(t+T)c_{n_1}^*(t-T)c_{n_2}(t+T)d_{z,n_1}^*(\underline{p}+\Delta_z(-T))d_{z,n_2}(\underline{p}+\Delta_z(T))$$

For numerical calculations, it can be convenient to split a complex integrand into its phase and absolute value. Although this is typically done with the given formula, the coefficients remain complex and may exhibit rapidly oscillating phase behavior.

2.4   Strong Field Ionization

This section mostly follows [1]. While not directly necessary for this thesis, these terms are frequently encountered in the literature and are briefly mentioned here for completeness. Ionization can occur in different ways, depending on the laser parameters and the atom or material used. To distinguish these processes, several parameters must be defined. According to [8], strong field ionization primarily depends on three parameters: the photon energy, the binding potential, and the ponderomotive energy.

Ponderomotive Energy   The ponderomotive energy is defined as the cycle-averaged quiver energy of a free electron in an electromagnetic field [cite wikipedia]. Since harmonic motion is experienced by the particle, the time-averaged kinetic energy is given by

$$\frac{1}{2}m\omega^2 \left\langle x^2 \right\rangle = \frac{e^2 E^2}{4m_e \omega^2} = \frac{E^2}{4\omega^2}$$

Keldysh Parameter   The Keldysh parameter γ compares the ponderomotive energy with the ionization potential. It is defined as

$$\gamma = \sqrt{\frac{I_p}{2U_p}}$$

The ionization potential in the hydrogen atom is $I_p = 13.6\mathrm{eV} = 0.5\mathrm{au}$. Different regimes of ionization, each with distinct physical interpretations, can be defined based on the value of the Keldysh parameter.

2.4.1 Tunneling Ionization

This regime is typically characterized by $\gamma \ll 1$. Here, the laser pulse is sufficiently strong to distort the potential barrier. Alternatively, the tunneling regime can be defined as the regime where the quasi-static approximation holds, meaning the instantaneous ionization rate is entirely determined by the absolute value of the electric field at that time [1]. This allows the ionization rate for DC and AC fields in this regime to be calculated analytically [4].

$$\Gamma_{\text{SFA}}(t) \propto \exp\left(-\frac{2}{3}\frac{(2I_p)^{3/2}}{F}\right)$$

Here, F represents the peak of the electric field for an AC field.

2.4.2 Multiphoton Ionization

The regime where $\gamma \gg 1$ is commonly referred to as multiphoton ionization. This occurs when the field strength is significantly weaker than in the tunneling regime. In other words, the multiphoton regime can be defined as the regime where

$$\Gamma_{\text{SFA}}(t) \propto \mathbf{E}^{2N} \quad \text{with} \quad N = \frac{I_p}{E_e}$$

holds [6]. This process can be visualized as the electron gaining energy while remaining under the barrier, effectively being heated up. Unlike the tunneling regime, this process is non-adiabatic. For further details, refer to [6] and [8].

2.4.3 Intermediate Regime

This regime is particularly relevant for this thesis. The previous regimes describe limiting cases where the complementary process is negligible. However, in reality, a coexistence of both processes often occurs. In the intermediate regime, the tunneling process is no longer adiabatic. The potential barrier undergoes significant oscillations during the electron's tunneling time, allowing energy to be absorbed from the laser field while tunneling takes place.

3. Methods

This chapter is about introducing the methods used throughout the thesis. This includes numerical methods for solving or implementing some type of equation as well as more physical methods that are used for comparing results or get more meaning to the data.

For comparing and verifying the ionization rate from chapter 2, one needs to solve the TDSE numerically without any approximations. A reliable choice for comparing is by using the sampling method called TIPTOE [11] and comparing the ionization yield from both approaches. Especially for expanding an already existing model, it is important to compare and see if the changes of the model are going into the right direction.

3.1 Numerical Methods

To implement formula 2.2.3 we need to solve the TDSE in two different ways numerically in order to obtain the coefficients $c_n(t)$. For that I used two different methods (numerical/direct and ODE) each with its own advantages and disadvantages.

For numerically solving the TDSE without any approximations I used a solver called tRecX.

3.1.1 tRecX

tRecX is a C++ code for solving generalized inhomogeneous time-dependent Schroedinger-type equations in arbitrary dimensions and in a variety of coordinate systems [14]. Usually ionization is difficult for an numerical solver because the electron "leaves" the subspace of the bound states, making the calculations very time consuming. Further, the coulomb potential only decays as $1/r$ so there is the question of how to discretize the space and set the boundary conditions.

tRecX uses different techniques making it especially suitable for light atom interaction. For instance, with the method called "Infinite-range exterior complex scaling" after a certan distance from the nucleus the space gets complex scaled via a unitary transformation. One could imagine this the same way as an function can be analytically continued into the

complex plane. Further the wavefunction gets also "damped" by the complex scaled region so there is reflection at the boundary which could cause numerical problems [13].

Further, tRecX allows to specify the gauge in which the TDSE is solved, making it more flexible. This will be important later.

Throughout this thesis, tRecX was used for two things. First, the for solving the TDSE in the whole hilbertspace to obtain the coefficients $c_n(t)$ that are needed for the imporved SFA rate. For this, the sourcecode had to be modified to calculate the coefficients and store them in an appropiate format. For more details about the implementation, see chapter 4.

Second, as a reference within the TIPTOE experiment to evaluate the performance of the SFA rate with excited states (**??**).

3.1.2   ODE

To acess the coefficients of the wavefunction inside the subspace of the bound states I used the interaction picture and solved the resulting coupled system of differential equations. To implement the calculation, Python and the ODE solver from SciPy integrate called `solve_ivp` was used. The code can be found in the electronic appendix in the class `HydrogenSolver`. For more details about the implementation, see chapter 4.

3.2   TIPTOE

This section mostly follows [11] and [1].

TIPTOE (Tunneling Ionization with a Perturbation for the Time-domain Observation of an Electric field) is a method for direct sampling of an electric pulse in the femtosecond to attosecond regime using quasistatic subcycle tunneling ionization in a gaseous medium or air.

A typical TIPTOE simulation consists of two linearly polarized laser pulses: a "fundamental" and a "signal" pulse, similar to common pump-probe experiments. The drive pulse is the pulse to be sampled, with the ionization yield of a certain medium providing the measurement. In first order, the ionization rate can be approximated as

$$\Gamma(E_F + E_S) \approx \Gamma(E_F) + E_S \left. \frac{d\Gamma(E_S)}{dE} \right|_{E=E_F} \tag{3.1}$$

In this approximation, depletion of the ground state is neglected. The total ionization yield N obtained by the two pulses is given by

$$N_{\text{total}} = N_0 + \delta N = \int dt, \Gamma(E_F(t)) + \int dt, E_S(t) \left. \frac{d\Gamma(E_S(t))}{dE} \right|_{E=E_F(t)}$$

By varying the delay τ between the two pulses, the ionization yield takes on different values. From this, it follows that:

$$\delta N(\tau) \propto E_{\mathrm{S}}(\tau) \tag{3.2}$$

Thus, the field amplitude of the signal pulse can be sampled by measuring the ionization yield for different delays. The TIPTOE method can be applied across a broad spectral range of the signal pulse, as long as the fundamental pulse is shorter than 1.5 optical cycles.

This method provides a way to compare ionization dynamics predicted by a numerical solver and by the SFA rate (**??**). TIPTOE is particularly useful because numerical simulations can provide good predictions about ionization probabilities, while analytical models describe ionization rates. A TIPTOE simulation can help reconstruct the ionization dynamics, which is especially relevant in the context of this thesis. Later, the ionization rate $\Gamma(E_{\mathrm{F}} + E_{\mathrm{S}})$ will be integrated over the full time domain, and the ionization yield for different delays will be compared with the results from the numerical solution of the TDSE. The results are shown in chapter 5.

For better visualization of the underlying physics in TIPTOE, the "background" ionization from $E_{\mathrm{F}}(t)$ is subtracted, and the ionization yield is normalized, so the formula in plot ???? reads

$$\frac{N_{\mathrm{total}} - N_0}{N_{\mathrm{max}}} = \frac{\delta N(\tau)}{N_{\mathrm{max}}}$$

However, interesting physics can also be observed by comparing the net ionization yield N_{total}, as discussed later in Chapter 5.

Typically, TIPTOE is not used for this kind of analysis but rather for its sampling capabilities. Instantaneous ionization rates are highly useful because TIPTOE enables sampling of the electric field of a laser pulse in the femtosecond to attosecond regime, which has broad applications in fields such as laser spectroscopy and medical physics.

3.3 GASFIR

GASFIR is short for general approximator for strong field ionization rates. It is an analytical retrieval tool for reconstructing data obtaned from numerical solutions of the TDSE. It was validated for hydrogen and shows good agreement with existing theories in the quasi static limit of tunneling ionization not only for Hydrogen, also for Helim and Neon [3]. The way how GASFIR works is that it uses ionization probabilities to retrieve ionization rates. It uses the idea from SFA that the rates can be written as $\int \mathrm{d}T\, K(t, T)$ with $K(t, T)$ being a kernel function. Later in the code you see also the kernel function, where the modifications happened. GASFIR is not a part of this thesis, it was motivated by the idea that an improvement of the SFA formalism could benefit the GASFIR approach.

4. Implementation

In this chapter I will explain how I implemented formula (2.2.3) in the code. Most of the code was already written by the authors of [2]. The exact changes I made can be found in the electronic appendix. Since I am using git, you can also see the changes in the commit history. The main two parts that where new in this implementation now are the coefficients $c_n(t)$ and the dipole matrix elements $\mathbf{d}_n(\underline{p})$.

4.1 Coefficients

As mentioned in chapter 2, there are two ways to write the dyson equation which results in two different expressions for the s-matrix. The only difference between both approaches are the coefficients. The ODE coefficients are with respect to the subspace spanned by the bound states, while tRecX coefficients are with respect to the full Hilbert space.

4.1.1 ODE

To see how to solve for the coefficients,, lets look at the defining equation again:

$$\hat{\mathcal{U}}_0^{\mathrm{ODE}}(t', t_0) \left| \Psi_0(t_0) \right\rangle = \sum_n c_n(t') e^{-iE_n t'} \left| \Psi_n \right\rangle$$

with

$$i\partial_{t'} \hat{\mathcal{U}}_0^{\mathrm{ODE}}(t', t_0) = \hat{X}\hat{\mathcal{H}}(t')\hat{X}\,\hat{\mathcal{U}}_0^{\mathrm{ODE}}(t', t_0) \tag{4.1}$$

One can think of it as the wavefunction is not "allowed" to leave the subspace. Lets do the derivation for the coefficients real quick.

We start by splitting the $\hat{\mathcal{H}}(t)$ into two parts $\hat{\mathcal{H}}_0$ and $\hat{\mathcal{H}}_{\mathrm{I}}(t)$ where the eigenstates of $\hat{\mathcal{H}}_0$ are $\{\left| \Psi_n \right\rangle\}$ and the eigenenergies $\hat{\mathcal{H}}_0$ are $\{E_n\}$. The next step is to plug the ansatz above into (4.1) and multiply with $\left\langle \Psi_m \right|$ to get the coefficients $c_n(t)$.

$$i\dot{c}_m(t) = \sum_n c_n(t) e^{-i\omega_{nm}t} \left\langle \Psi_m | \hat{\mathcal{H}}_{\mathrm{I}}(t) | \Psi_n \right\rangle$$

with $\omega_{nm} = E_n - E_m$.

Now this has its problems. First, $\sum_n$ goes from 0 to ∞, but since we are in numerical simulations we have to limit ourselves to a finite number of states. How can we justify the number choosen? How can we make shure that the abrubt end of the sum does not cause any numerical problems?

One way to think about it is just testing. By increasing the number of states used in the sum, the results (i.e. the rates) should converge. However, since we forced the electron to stay inside the subspace, going to higher and higher excited states can cause numerical problems as well. Especially for higher intensities and longer wavelengths, going to higher states caused unphysical oscillations in the rates. Eventually one has to find a certain number of states that is precise enough but does not cause numerical problems. For my simulations later, I used a maximum of $n = 3$ for the calculation of the bound states. One could justify that by looking at the population; most of the dynamics before ionization is determined by the first few bound states, especially $1s$, $2s$, $2p$ and $3p$ so solving for more doesnt affect the previous coefficients not much.

Note: This was not about how many bound states I include in the final simulations, but how many I even considered when solving the ODE. I could have used only the ground state in the SFA rate later on, but there is still the question how many bound states have an effect on the ground state. This number was justified here.

Further, equation (4.1.1) is gauge dependent because of $\langle m|\hat{\mathcal{H}}_{\mathrm{I}}(t)|n\rangle$. We can either choose length gauge (2.8) or velocity gauge (2.9). Which gauge should we use to get the most meaningful results?

To answer this question, lets think about the scenario again. An electron sits in ground state and bevore ionization its behavior is mainly described by the coulomb potential. After it gets ionized, SFA tells us it is now described as a plane wave oscillating in the laser pulse.

With this in mind, we can see that both gauges can be usefull. During the first part of the process, i.e. the electron being still bounded to the hydrogen atom, the length gauge is more appropiate since most of the behavior of the electron can be described better when knowing more about the position of the electron rather then its momentum. That is why in most elementary introductions on light matter interaction (for instance with rabi socillations and so on) length gauge because the system can not ionize. On the other hand, after ionization it is better to use velocity gauge since there is no potential anymore (because of SFA) and the elcetron is fully described by its momentum.

This makes length gauge a fitting candidate for the coefficients used in the ODE ansatz.

4.1.2   tRecX

The coefficients from the ODE are not the only one im using. I used tRecX to calculate solve the entire TDSE and extract the coefficients from the whole wavefunction. As mentioned earlier, there are two ways to think about $\hat{\mathcal{U}}(t', t_0)\,|\Psi\rangle$. First, solve the TDSE in the subspace of the bound states (we did that with the ODE) or solve the TDSE in the full Hilbert space and the project it onto bound states. tRecX does the second one, which is far more complicated than what I did using the ODE. However, tRecX results are also gauge dependent, so we need to be careful with the gauge. Also it is far more difficult to interpret the rsults from tRecX since many effects can determine the time evolution of the coefficients and therefore the ionization rate but its of course helpfull to have two independent sources of in some sense the same thing.

4.1.3   Coefficients

For initial values `c_n(0) = 1` for the ground state and `c_n(0) = 0` for all other states were choosen. In theory, $|c_n(t)|^2$ or the amplitude of the coefficients is observable quantity and can be measured in experiment. It tells us how propable the system is to be in a certain state n at time t. Furthermore, and most importantly, they are gauge independent. But since SFA is gauge dependent theory, and now we are not even dealing with the amplitude instead the complex coefficients, we need to be extremely careful with the gauge.
In my thesis there are mostly two gauges used, the length gauge and the velocity gauge. In the following plot you see that the amplitudes are indeed not gauge independent. But why is that the case?

The gauge is a very fundamental problem. Not so fundamental is our ansatz, as mentioned erlier we artificially force the electron to stay in the part of the Hilbert space covered by the bound state. This restricts us to small ionization propabilities, and may also cause some numerical problems as will discussed later.
Also the numerical issue that we need to have infinitely many bound states for covering the aprt of the Hilbert space completely is not possible, so we have to limit ourselves. First this seems like a big problem, but we will see that most of the dynamics inside the electron before ionisation is in my simulations only determined by a few bound states. But one still need to be carefull with the number of used bound states, but because of numerical reasons.

For my numerica solution I used a system of ordinary differential equations (ODEs) to

calculate the coefficients $c_n(t)$ using the interaction picture. In my implementation I neglected transitions to states that are forbidden via the dipole selection rules. However this is an approximation, since in reality two-photon processes can occur, effectively allowing transitions between $1s$ and $2s$ for instance. I numerically solved the schroedinger equation with tRecX and modyfied the code to print out the coefficients $c_n(t)$ allowing me to get insight in the "real" dynamics of the electron.

Question: how many cound states do we nodd (mentioned earlier)?

in E4 it was easy because laser had cosine shape. attosecond physics not the case, more a lase pulse, cos8 envelope so it doesnt make much sense to speak of rabi oszillations.
I also need to check how often I have to write the coefficients to the expec file. That depends on the characterisitc time of the state and on the frequency of the laser of course.
Naiv: as much as possible to be precise as possible. But: we dont want to exceed the length gauge regime, are best described in length not velocity gauge. Further: more phenomenological but most of the dynamics is int the first few bound states, like 2s, 2p, 3p thats mostly it. For that just look at the $|c_n(t)|^2$ which has the highest amplitudes.

For extracting the coefficients from tRecX so solving the full TDSE and then projecting onto bound states I modifyed the code as following: Already implemented was the Occupation propability of specified bound states, so the code prints out $\langle \Psi(t)|\hat{P}_{\text{Occ}\{\text{H0:n}\}}{}^1|\Psi(t)\rangle = |\langle\Psi(t)|n\rangle|^2$ In principle all I did was changing implementing a new function that changes the left bra $\langle\Psi(t)|$ to the eigenstate used in $\hat{P}_{\text{Occ}\{\text{H0:n}\}}$ and verifying that the eigenstates are normalized. This gives us

$$\langle\Psi(t)|\hat{P}_{\text{Occ}\{\text{H0:n}\}}|\Psi(t)\rangle \rightarrow \langle n|\hat{P}_{\text{Occ}\{\text{H0:n}\}}|\Psi(t)\rangle = \langle n|n\rangle \times \langle n|\Psi(t)\rangle = c_n(t)$$

For that I needed to solve the eigenvalueporblem again, and pass the eigenstates down to the function calculating the expectation value. There is defenitely a more elegant way to do that, especially efficiency wise, since the eigenstates are already calculated elsewhere, but for now this works.

4.1.4   Dipole matrix Elements

$m = 4$ because light linear polarized!!!! The dipole matrix elements are an essential part of the formula in (2.2.3). Calculating it generall is difficult, but in the case of hydrogen its even possible to do it analytically A. However, its that easy to calculate because we made a very coarse approximation, since the final state after ionisation is not in realtiy a plane

wave, but we approximated it with that by using SFA.

Furthermore, our problem is

For the dipole matrix elements its alsow needed to simplify them as much as possible. Sometimes certain parts cancel out later in the integration (phi integral) but the computer is not good with that, even some small numerical errors will cause it to be not exactl zero and messes up the calculation.

4.2   tRecX TIPTOE Simulations

4.2.1   TIPTOE

TIPTOE [11] is a sampling method used for sub femtosecond processes. It is relevant for this thesis because it was used to verify the results from the Ionization model. TIPTOE is great because its fundamentals are very simple but it can tell you a lot about the dynamics in attosecond regime.

Now i used length gauge for the coefficients but velocity gauge for the ionization propabilities

5. Results and Discussion

Before discussing the results, first we have to formulate what we want to learn from this kind of generalisation. The main difference form previous literatuee was the use of transition to excited states before ionisation. In principle we want to investigate how this tranistion influeces the ionisation process or in general the ionisation rate.

Previously: time reversal symmetry, what causes it?

Also we want to know what influences the ionization rate more, the stark shift or the distortion of the ground state.

Also we want to get closer to the tRecX TIPTOE results because thats all we really got (quantum mechanics fundamentals) maybe including excited states will help us.

All results are stored in a github repository and can be reproduced.

5.1 Stark Shift

The Stark effect is the shift of the energy levels of an atom or molecule due to the presence of an external electric field.
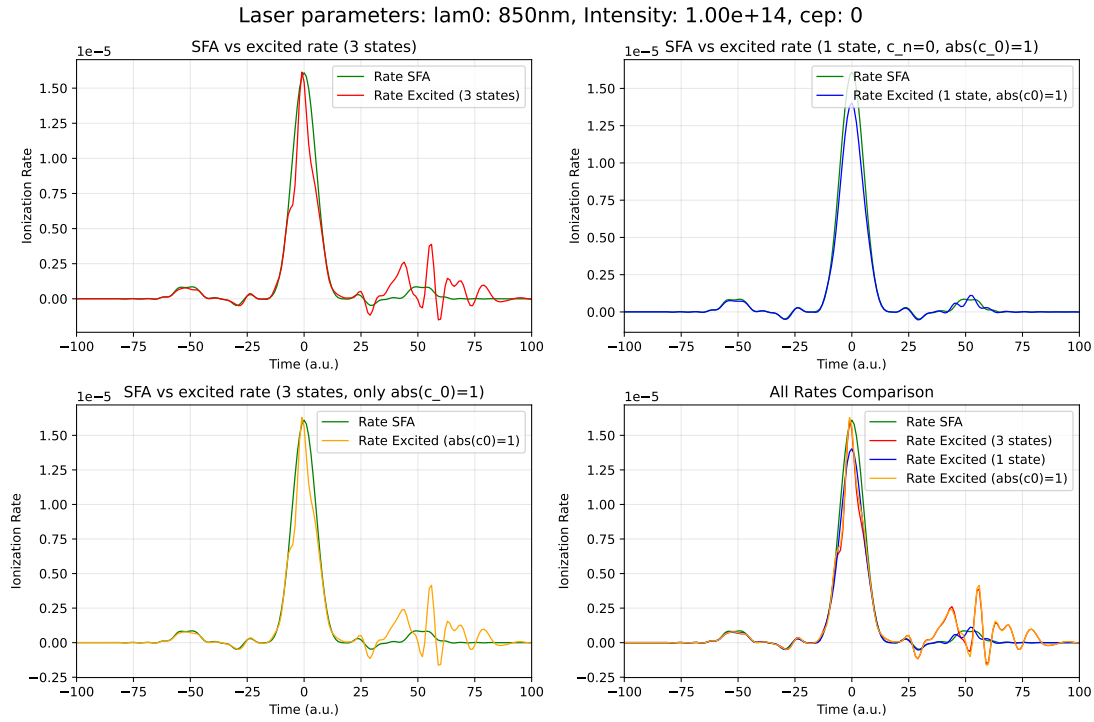
Figure 5.1: stark effect

Naiv: Stark effect changes energy in electron so its "harder" to ionise, thats why blue curve goes down (when excitedStates=1). But thats not certainly the case because of stark effect, thats why only set absc0 to 1 and phase remains. Example with oszillations with time dependent resonance frequency, and external force not at resonance but coincidence with oszillator resonance frequency so this may cause it.

5.2   Rates

Stark shift doesnt seem to have much contribution (sadly) but at least more than the polarisation of the ground state.

Lets investigate the influence of first coefficient, nothing more. Only the phase has a contribution, the amplitude is not important. Thats because the amplitude determines something occupation propabilitiy, but the phase is e^{-iEt} and if E is shifted by a bit you can isolate it by just using purely the phase.
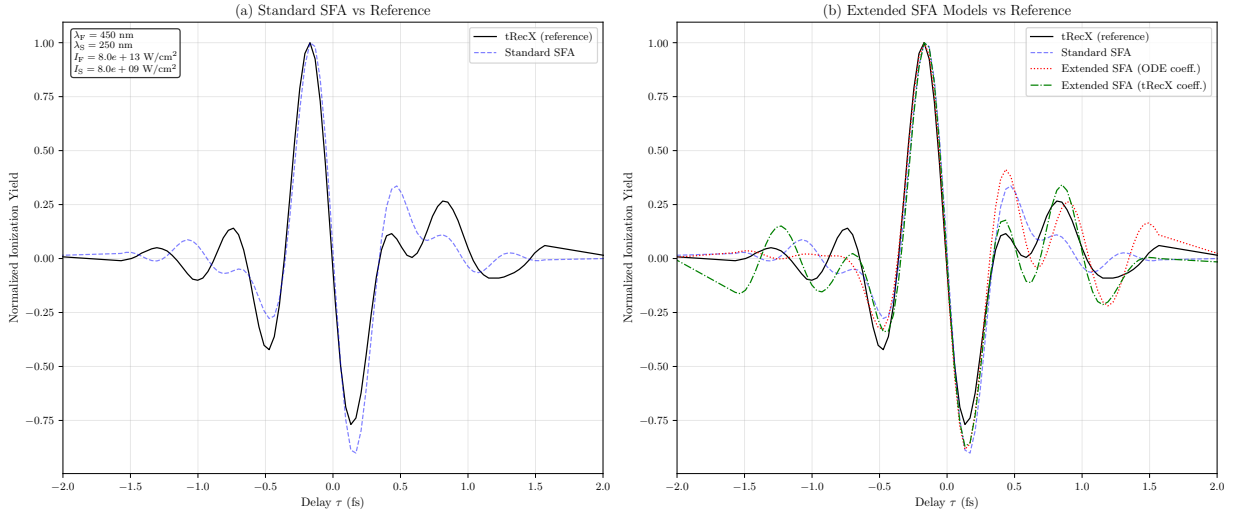
Top right is the isolated stark effect

Figure 5.2: Comparison of ionization yields from TIPTOE simulations between different SFA models and reference data from tRecX. (a) Standart SFA overall does a good job reconstructing the ionization dynamics, but some parts it does not capture at all (b) Extended SFA to excited states indeed shows some improvements in the reconstructing

5.3 TIPTOE

From the TIPTOE results we want to learn, weither the tRecX coefficients or the SFA coefficients bring us closer to the tRecX ionProb results and if excited states help at all.

Note that (3.2) is fulfilled and it actually looks like the signal pulse. On the left plot we see that tRecX is still orders of magnitude larger than the SFA results. However, with excited states it goes in the right direction as can be seen on the right plot. For three excited sates there is not much imporvement visible. Unfortunately, the results are no where close to the tRecX measurements. That indicates that there is some physics missing in the SFA model. If its not the excited states, the it must be something else. And because the change is so big it has to be something more fundamental. The first idea is that the interaction with the coulomb potential after ionization cannot be completely neglected, as it is done in the SFA model. Even though it is counterintuitive, becasue if the coulomb potential is still noticable for the electron after ionization, why would it increase the results we are seeing?????? But this is in principle what our simulations are telling us. We can argue that we have two different ways of calculating the coefficients (ODE and tRecX) and the reproduce the same result.

However it indicates that real ionization propabilities do have some characterisitcs that the improved SFA model does not capture.

One also should make clear what the ODE coefficients do not capture. First, I imple-

mented the code such that it ignores transitions not allowed by the dipole selection rules.

So in principle, assuming my SFA modification was correct the TIPTOE results tell us that the coulomb potential is not negligible after all. Maybe because the laser is not that intense (multiphoton ionization). But its difficult to test that because if I increase the laser intensity, the approximations I made with the coefficients is not valid anymore.

Looking at not normalized results, tRecX is much more sensitive to the shift of probe and pump pulse, while excited SFA coefficients are not Maybe because tRecX takes into account all the dynamics and effects inside an atom, while excited SFA coefficients does not care that much. I would expect with tRecX coefficients more sensitive than with ODE coefficients???

5.4   Lorem

This might be how it is supposed to be – we are in the regime where the laser field is strong enough to ionize the atom, but we artificially force the electron to stay in the part of the Hilbert space covered by a few bound states. If the calculations are converged with respect to the time step, and you see convergence regarding the number of bound states in the weak-field regime, then it's fine if there is no convergence with respect to the number of bound states in the strong-field regime.

6. Conclusion and Outlook

Could be good for GASFIR because GASFIR learns from exact SFA rate.
What is more important, stark shift or else?

Lorem ipsum dolor sit amet, consetetur sadipscing elitr, sed diam nonumy eirmod tempor invidunt ut labore et dolore magna aliquyam erat, sed diam voluptua. At vero eos et accusam et justo duo dolores et ea rebum. Stet clita kasd gubergren, no sea takimata sanctus est Lorem ipsum dolor sit amet. Lorem ipsum dolor sit amet, consetetur sadipscing elitr, sed diam nonumy eirmod tempor invidunt ut labore et dolore magna aliquyam erat, sed diam voluptua. At vero eos et accusam et justo duo dolores et ea rebum. Stet clita kasd gubergren, no sea takimata sanctus est Lorem ipsum dolor sit amet.

A. Dipole transition matrix elements

We want to derive the general transition dipole matrix elements into the continuum for an hydrogen-like atom. The general matrix element in our case is given by:

$$\underline{d}_{nlm}(\underline{p}) = \langle \Pi | \hat{\mathbf{d}} | \Psi_{nlm} \rangle \overset{\text{a.u.}}{=} \langle p | \hat{\mathbf{r}} | \Psi_{nlm} \rangle$$

With $|p\rangle$ being a plane wave. By partitioning the $\hat{\mathbf{1}}$, and using the fact that $\hat{\mathbf{r}} \to i\nabla_{\underline{p}}$ in momentum representation we find a generel formula for the transition:

$$\underline{d}_{nlm}(\underline{p}) = i\nabla_{\underline{p}} \int \mathrm{d}^3\underline{x}\, \psi_{nlm}(\underline{x}) e^{-i\underline{p}\cdot\underline{x}} = i\nabla_{\underline{p}}\phi_{nlm}(\underline{p})$$

In principle, this integral or more precise the Fouriertransformation of the wavefunction is all we need to do. Because of the structure of ψ_{nlm} we can expect a result simular to (eqref psi=RY). A posteriori we will see that:

$$\mathcal{F}\{\psi_{nlm}(\underline{x})\} = \phi_{nlm}(\underline{p}) = F_{nl}(p)Y_{lm}(\theta_p, \phi_p)$$

With $F_{nl}(p)$ being the Fouriertransform of the radial part of the wavefunction and $Y_{lm}(\theta_p, \phi_p)$ being the spherical harmonics in momentum space similar to the hydrogen atom in position space.

Momentum space

We start with the so called plane wave expansion [7] of the exponential part of the integral:

$$e^{i\underline{p}\cdot\underline{x}} = \sum_{l'=0}^{\infty}(2l'+1)i^{l'}j_{l'}(pr)P_{l'}(\underline{p}\cdot\underline{x}) = 4\pi\sum_{l'=0}^{\infty}\sum_{m'=-l'}^{l'}i^{l'}j_{l'}(pr)Y_{l'm'}(\theta_p, \phi_p)Y_{l'm'}^{*}(\theta_x, \phi_x)$$

With $j_l(pr)$ being the spherical bessel functions. Also note that we are integrating over spherical kordinates now. At first it looks messy but we can use the orthogonality of the

spherical harmonics we can reduce the integral to:

$$\phi_{nlm}(\underline{p}) = 4\pi \sum_{m=-l}^{l} Y_{lm}(\theta_p, \phi_p) i^l \underbrace{\int_0^\infty \mathrm{d}r\, r^2 j_l(pr) R_{nl}(r)}_{\tilde{R}_{nl}(p)}$$

This is the structure we were hoping for. Lets focus on the radial part $\tilde{R}_{nl}(p)$ of the integral. The term $R_{nl}(r)$ represents the radial function of the hydrogen atom in position space and is independent of the magnetic bumber m. An exponential term dependent of r, a polynomial term dependent of r, the generalized Laguerre polynomials and the normalization constant. It would be convenient to have a closed expression for the generalzied Laguerre polynomials. I choose to represent them as following:

$$L_n^l(r) = \sum_{\iota=0}^{n} \frac{(-1)^\iota}{\iota!} \binom{n+l}{n-\iota} r^\iota$$

The Laguerre polynomials are therefore only dependent on and exponential term and finitely many polynomial terms. $\tilde{R}_{nl}(p)$ can be expressed (without prefactors and summation over ι) as:

$$\int_0^\infty \mathrm{d}r\, r^{2+l+\iota} e^{-\frac{Zr}{n}} j_l(pr)$$

Before we can solve the Integral using caomputational methods, we need to transform the spherical bessel function into the ordinary ones:

$$j_l(pr) = \sqrt{\frac{\pi}{2pr}} J_{l+\frac{1}{2}}(pr)$$

Now it is a good time to write all the prefactors and summations in one expression and look at the integral as a whole:

$$\phi_{nlm}(\underline{p}) = \frac{\pi^{3/2}}{\sqrt{2p}} \sqrt{\left(\frac{2}{n}\right)^3 \frac{(n-l-1)!}{n(n+1)!}}$$

$$\times \sum_{m=-l}^{l} \sum_{\iota=0}^{n-l-1} i^l \frac{(-1)^\iota}{\iota!} \left(\frac{2}{n}\right)^{l+\iota} \binom{n+l}{n-l-1} \underbrace{\int_0^\infty \mathrm{d}r\, r^{l+\iota+\frac{3}{2}} e^{-\frac{Zr}{n}} J_{l+\frac{1}{2}}(pr)}_{(*)} Y_{lm}(\theta_p, \phi_p)$$

To calculate the remaining Integral, I used mathematica, so I can not give a detailed explanation of that. Interestingly, there is an analytical solution for that. The result for $(*)$ is:

$$(*) = {}_2\tilde{F}_1 \left(2+l+\frac{\iota}{2}, \frac{1}{2}(5+2l+\iota); \frac{3}{2}+l; -\frac{n^2 p^2}{Z^2}\right)$$

With $_2\tilde{F}_1$ being the regularized hypergeometric function defined by:

$$_2\tilde{F}_1(a,b;c;z) = \frac{_2F_1(a,b;c;z)}{\Gamma(c)} = \frac{1}{\Gamma(a)\,\Gamma(b)} \sum_{n=0}^{\infty} \frac{\Gamma(a+n)\,\Gamma(b+n)}{\Gamma(c+n)} \frac{z^n}{n!}$$

The final formula $\phi_{nlm}(\underline{p})$ that can be also found in [atoms and molekulse] in slightely different form, can then be expressed as:

$$
\begin{aligned}
\phi_{nlm}(\underline{p}) = \sum_{\iota=0}^{2l+1} & \frac{(-1)^\iota \, 2^{\iota+\frac{1}{2}} \, n \, (in)^l \, (p^2)^{l/2} \, Z^{-l-3} \, \Gamma(2l+\iota+3)}{\iota!} \\
& \times \begin{pmatrix} l+n \\ -l+n-\iota-1 \end{pmatrix} \sqrt{\frac{Z^3 \Gamma(n-l)}{\Gamma(l+n+1)}} \\
& \times Y_l^m(\theta_p, \phi_p) \, _2\tilde{F}_1\left(l+\frac{\iota}{2}+2, \frac{1}{2}(2l+\iota+3); l+\frac{3}{2}; -\frac{n^2 p^2}{Z^2} \right)
\end{aligned}
\tag{A.1}
$$

Improved rate

Usually all thats left is to differentiate (A.1) with respect to $\underline{p}$. However, before that it is possible to directly improve the SFA rate by doing the integration over θ_p and ϕ_p analytically. The rate according to chapter 2 is given by:

$$
\begin{aligned}
\Gamma_{\text{SFA}}(t) = \sum_{n_1} \sum_{n_2} & \int_0^\infty \mathrm{d}p \, p^2 \int_0^\pi \mathrm{d}\theta_p \, \sin\theta_p \int_0^{2\pi} \mathrm{d}\phi_p \int_{-\infty}^\infty \mathrm{d}T \\
& \times \exp\left(i\mathbf{p}^2 T + ip\cos\theta_p \bar{\Delta}_z^k + \frac{i}{2}\bar{\Delta}_z^2 + i(t-T)E_{n_1} - i(t+T)E_{n_2} \right) \\
& \times E_z(t-T)E_z(t+T)c_{n_1}^*(t-T)c_{n_2}(t+T)d_{z,n_1}^*(\underline{p}+\Delta_z(-T))d_{z,n_2}(\underline{p}+\Delta_z(T))
\end{aligned}
$$

As mentioned before the dipole transition matrix element can be written in the following form convenient form:

$$d_{z,nlm}(\underline{p}) = \left[i\nabla_{\underline{p}}\phi_{nlm}(\underline{p}) \right]_z = iY_{lm}(\theta_p, \phi_p)\left(\cos\theta_p \frac{\partial F_{nl}}{\partial p} - \frac{\sin\theta_p}{p}\frac{\partial F_{nl}}{\partial p} \right)$$

Note that here the z component of a gradient in spherical coordinates was taken. The exact formula can be easily computed using the transformation between cartesian and spherical coordinates.

The integration over θ_p is difficult and might be not possible to do analytically. However

for the integral over ϕ_p we only have to solve the following:

$$\int_0^{2\pi} \mathrm{d}\phi_p \, Y^*_{l'm'}(\theta_p, \phi_p) Y_{lm}(\theta_p, \phi_p) = \frac{1}{4\pi}\sqrt{(2l+1)(2l'+1)\frac{(l-m)!(l'-m')!}{(l+m)!(l'+m')!}} \int_0^{2\pi} \mathrm{d}\phi_p \, e^{i(m-m')\phi_p}$$

$$= \frac{1}{2}\sqrt{(2l+1)(2l'+1)\frac{(l-m)!(l'-m)!}{(l+m)!(l'+m)!}}$$

Further since only the z component of the gradient is important only the partial derivative of $\phi_{nlm}(\underline{p})$ with respect to p is needed. This can be also done analytically.

$$\frac{\partial F_{nl}(p)}{\partial p} = \sum_{\iota=0}^{2l+1} \frac{(-1)^\iota \, 2^{\iota+\frac{1}{2}} \, n \, (in)^l \, Z^{-l-3} \, \Gamma(2l+\iota+3)}{\iota!}$$

$$\times \begin{pmatrix} l+n \\ -l+n-\iota-1 \end{pmatrix}\sqrt{\frac{Z^3\Gamma(n-l)}{\Gamma(l+n+1)}}$$

$$\times \left(lp^{l-1}{}_2\tilde{F}_1\left(l+\frac{\iota}{2}+2, \frac{1}{2}(2l+\iota+3); l+\frac{3}{2}; -\frac{n^2p^2}{Z^2}\right)\right.$$

$$\left.\times \frac{p^l n^2}{Z^2}{}_2\tilde{F}_1\left(l+\frac{\iota}{2}+1, \frac{1}{2}(2l+\iota+1); l+\frac{1}{2}; -\frac{n^2p^2}{Z^2}\right)\right)$$

Transition Element

Now all thats left is to differentiate (A.1) with respect to $\underline{p}$.

new eq

$$\sum_{\iota=0}^{2l+1}\left(-\frac{(-1)^\iota n \mathrm{Ip}^{-l-3}2^{\iota-l-1}(in)^l (p^2)^{l/2}\left(\frac{1}{\sqrt{p^2}} - \frac{\mathrm{pz}^2}{(p^2)^{3/2}}\right)\Gamma(2l+\iota+3)\begin{pmatrix} l+n \\ -l+n-\iota-1 \end{pmatrix}\sqrt{\frac{\mathrm{Ip}^3\Gamma(n-l)}{\Gamma(l+n+1)}}{}_2\tilde{F}_1\left(l+\frac{\iota}{2}+2, \frac{1}{2}(2\right.}{}\right.$$

$$\tag{A.2}$$

$$
\sum_{\iota=0}^{2l+1} \Bigg(- \frac{(-1)^\iota n\, \mathrm{Ip}^{-l-3} 2^{\iota-l-1}(in)^l (p^2)^{l/2}\left(\frac{1}{\sqrt{p^2}} - \frac{\mathrm{pz}^2}{(p^2)^{3/2}}\right)\Gamma(2l+\iota+3)\binom{l+n}{-l+n-\iota-1}\sqrt{\frac{\mathrm{Ip}^3\Gamma(n-l)}{\Gamma(l+n+1)}}}{\iota!\sqrt{1-\frac{\mathrm{pz}^2}{p^2}}}
$$

$$
\times\ {}_2\tilde{F}_1\left(l+\frac{\iota}{2}+2, \frac{1}{2}(2l+\iota+3); l+\frac{3}{2}; -\frac{n^2 p^2}{4\mathrm{Ip}^2}\right)\left(\frac{m\,\mathrm{pz}\, Y_l^m\left(\cos^{-1}\left(\frac{\mathrm{pz}}{\sqrt{p^2}}\right),\tan^{-1}(\mathrm{px,py})\right)}{\sqrt{p^2}\sqrt{1-\frac{\mathrm{pz}^2}{p^2}}}\right.
$$

$$
\left.+\frac{\sqrt{\Gamma(l-m+1)}\sqrt{\Gamma(l+m+2)}e^{-i\tan^{-1}(\mathrm{px,py})}Y_l^{m+1}\left(\cos^{-1}\left(\frac{\mathrm{pz}}{\sqrt{p^2}}\right),\tan^{-1}(\mathrm{px,py})\right)}{\sqrt{\Gamma(l-m)}\sqrt{\Gamma(l+m+1)}}\right)
$$

$$
+\frac{(-1)^\iota ln\,\mathrm{pz}\,\mathrm{Ip}^{-l-3}2^{\iota-l-1}(in)^l(p^2)^{\frac{l}{2}-1}\Gamma(2l+\iota+3)\binom{l+n}{-l+n-\iota-1}\sqrt{\frac{\mathrm{Ip}^3\Gamma(n-l)}{\Gamma(l+n+1)}}}{\iota!}{}_2\tilde{F}_1\left(l+\frac{\iota}{2}+2,\frac{1}{2}(2l+\iota+\right.
$$

$$
-\frac{(-1)^\iota n^3 \mathrm{pz}\,\mathrm{Ip}^{-l-5}2^{\iota-l-3}\left(\frac{\iota}{2}+l+2\right)(\iota+2l+3)(in)^l(p^2)^{l/2}\Gamma(2l+\iota+3)\binom{l+n}{-l+n-\iota-1}\sqrt{\frac{\mathrm{Ip}^3\Gamma(n-l)}{\Gamma(l+n+1)}}}{\iota!}{}_2\tilde{F}_1\Bigg(
$$

$$
\tag{A.3}
$$

B. Code

This is a part of the code used to implement the SFA rate, where the calculations actually take place. One can see the usage of the coefficients and the dipole transition elements.

```python
for state_idx in range(excitedStates):
    for state_range_idx in range(excitedStates):
        f0 = np.zeros((Tar.size, tar.size), dtype=np.cdouble)
        phase0 = np.zeros((Tar.size, tar.size), dtype=np.cdouble)
        cLeft = coefficients[state_idx, :]
        cRight = coefficients[state_range_idx, :]
        phaseleft = np.unwrap(np.angle(cLeft))
        phaseright = np.unwrap(np.angle(cRight))
        absleft = np.abs(cLeft)
        absright = np.abs(cRight)

        for i in prange(Tar.size):
            Ti=Ti_ar[i]
            for j in range(tar.size):
                tj=N+nmin+j*n
                tp=tj+Ti
                tm=tj-Ti
                if tp>=0 and tp<EF.size and tm>=0 and tm<EF.size:
                    VPt = 0
                    T= Ti*dT
                    DelA = (intA[tp] - intA[tm])-2*VPt*T
                    VP_p=VP[tp]-VPt
                    VP_m=VP[tm]-VPt
                    f_t_1= np.conjugate(transitionElement(config[state_idx], p, pz, VP_m, E_g))*
                        transitionElement(config[state_range_idx], p, pz, VP_p, E_g)
                    G1_T_p=np.trapz(f_t_1*np.exp(1j*pz*DelA)*np.sin(theta), Theta_grid)
                    G1_T=np.trapz(G1_T_p*window*p_grid**2*np.exp(1j*p_grid**2*T), p_grid)
                    DelA = DelA + 2 * VPt * T
                    phase0[i, j] = (intA2[tp] - intA2[tm])/2 + T*VPt**2-VPt*DelA +eigenEnergy[
                        state_idx]*tp*dT-eigenEnergy[state_range_idx]*tm*dT -phaseleft[tm]+
                        phaseright[tp]
                    f0[i, j] = EF[tp]*EF[tm]*G1_T*absleft[tm]*absright[tp]
        current_state_rate = 2*np.real(IOF(Tar, f0, (phase0)*1j))*4*np.pi
        rate += current_state_rate
    return rate
```

This is the main part where the tRecX coefficients are computed. It can be seen that in the `matrixElementUnscaled` method instead of computing $\langle \Psi(t)|\Psi_n\rangle\langle\Psi_n|\Psi(t)\rangle = |c_n(t)|^2$ the left side of expectation has been modifyed to $\langle\Psi_n|\Psi_n\rangle\langle\Psi_n|\Psi(t)\rangle = c_n(t)$.

```cpp
static std::complex<double> eigenProjection(int IOp, std::vector<OperatorAbstract*> Ops, double Time,
    const Coefficients* Wf, bool Normalize, std::vector<std::shared_ptr<Coefficients>> Duals){
    Ops[IOp]->update(Time,Wf);
    if (IOp > 1 && !Duals.empty() && IOp - 2 < Duals.size()) {
        const Coefficients* constdual_raw = Duals[IOp - 2].get();
        complex<double> expec=Ops[IOp]->matrixElementUnscaled(*constdual_raw,*Wf);
        expec=Threads::sum(expec);
        if(Normalize){
            std::complex<double> nrm=1.;
            if(Ops[IOp]->name().find("Ovr(")==std::string::npos){
                for(auto o: Ops){
                    if(o->name().find("Ovr(")!=std::string::npos){
                        nrm=Threads::sum(o->matrixElementUnscaled(*constdual_raw,*Wf));
```

```
13                          break;
14                      }
15                  }
16              }
17          if(nrm!=0.) expec/=nrm;
18      }
19      return expec;
20  }
```

Bibliography

[1] Manoram Agarwal. A theory of photoconductive sampling of optical fields in atomic gases. Master's thesis, Ludwig-Maximilians-Universität München, 2022.

[2] Manoram Agarwal, Armin Scrinzi, Ferenc Krausz, and Vladislav S. Yakovlev. Theory of nonlinear photoconductive sampling in atomic gases. *Annalen der Physik*, 535(12):2300322, 2023.

[3] Manoram Agarwal, Armin Scrinzi, and Vladislav S. Yakovlev. A general approximator for strong-field ionization rates, 2025.

[4] Maxim V Ammosov, Nikolai B Delone, and Vladimir P Krainov. Tunnel Ionization Of Complex Atoms And Atomic Ions In Electromagnetic Field. In John A. Alcock, editor, *High Intensity Laser Processes*, volume 0664, pages 138 – 141. International Society for Optics and Photonics, SPIE, 1986.

[5] Lea Boßmann. On the dipole approximation, 2016.

[6] Misha Yu Ivanov, Michael Spanner, and Olga Smirnova and. Anatomy of strong field ionization. *Journal of Modern Optics*, 52(2-3):165–184, 2005.

[7] John David Jackson. *Classical Electrodynamics*. Wiley, 1998.

[8] L. V. Keldysh. Ionization in the Field of a Strong Electromagnetic Wave. *J. Exp. Theor. Phys.*, 20(5):1307–1314, 1965.

[9] L. D. Landau and E. M Lifschitz. *Band 2 Klassische Feldtheorie*. De Gruyter, Berlin, Boston, 1976.

[10] A. Ludwig, J. Maurer, B. W. Mayer, C. R. Phillips, L. Gallmann, and U. Keller. Breakdown of the dipole approximation in strong-field ionization. *Phys. Rev. Lett.*, 113:243001, Dec 2014.

[11] Seung Beom Park, Kyungseung Kim, Wosik Cho, Sung In Hwang, Igor Ivanov, Chang Hee Nam, and Kyung Taec Kim. Direct sampling of a light wave in air. *Optica*, 5(4):402–408, Apr 2018.

[12] José Luis Sanz-Vicario and Carlos Mario Granados-Castro. Time-dependent feshbach method to study resonant photoionization of he with ultrashort laser pulses. In *Journal of Physics: Conference Series*, volume 488, page 012018. IOP Publishing, 2014.

[13] Armin Scrinzi. Infinite-range exterior complex scaling as a perfect absorber in time-dependent problems. *Phys. Rev. A*, 81:053845, May 2010.

[14] Armin Scrinzi. trecx — an environment for solving time-dependent schrödinger-like problems. *Computer Physics Communications*, 270:108146, January 2022.

Declaration of Authorship

Hiermit erkläre ich, die vorliegende Arbeit selbständig verfasst zu haben und keine anderen als die in der Arbeit angegebenen Quellen und Hilfsmittel benutzt zu haben.

München, den 20.6.2025

_____

Unterschrift